2023 IEEE/RSJ International Conference on Intelligent Robots and Systems (IROS)
October 1-5, 2023. Detroit, USA

A Fabrication and Simulation Recipe for Untethering Soft-Rigid Robots with Cable-Driven Stiffness Modulation

James M. Bern*,1,2, Zach J. Patterson*,2, Leonardo Zamora Yañez[2], Kristoff K. Misquitta[2], and Daniela Rus[2]

***Abstract*— We explore the idea of robotic mechanisms that can shift between soft and rigid states, with the long-term goal of creating robots that marry the flexibility and robustness of soft robots with the strength and precision of rigid robots. We present a simple yet effective method to achieve large and rapid stiffness variations by compressing and relaxing a flexure using cables. Next, we provide a differentiable modeling framework that can be used for motion planning, which simultaneously reasons about the modulated stiffness joints, tendons, rigid joints, and basic hydrodynamics. We apply this stiffness tuning and simulation recipe to create SoRiTu, an untethered soft-rigid robotic sea turtle capable of various swimming maneuvers.**

I. Introduction

For the last decade, the soft robotics community has developed many soft-bodied and highly flexible machines under the premise that these morphologies can make such robots safe for interaction with humans and their environments and, more subtly, that they will help to reduce the need for precise state estimation [1], [2]. This overall line of work was motivated in part by the rich examples of specialized soft structures that have been observed in the animal kingdom, including in several terrestrial organisms [3], [4] and many aquatic invertebrates [5], [6].

While soft robotics has yielded many promising results [7], purely soft passive structures struggle to transmit large loads [8] or operate with high precision. This makes sense from a biological perspective, as many of the creatures we seek inspiration from are *vertebrates*, which make use of rigid structures to aid in locomotion and environmental interaction. Furthermore, it has been famously observed that the octopus, although its arms lack bones, still manifests elbow-liked "joints" to accomplish precision tasks [9], [10].

Inspired by such ideas, we are interested in developing robots that utilize both soft and rigid structures and that are able to modulate between soft and rigid states, a concept often referred to (both in robotics and materials science) as "stiffness tuning" [11]. Such robots have the potential to help in human-centric domains, which demand both delicacy and high load-bearing capacity [12]–[14]. In this work, we continue our exploration of soft-rigid shape-shifting, and present the fabrication, simulation, and application of a 3D-printed joint mechanism offering fast and dramatic cable-driven stiffness modulation.

The presented mechanism is an instance of cable-driven jamming and structure-based stiffness tuning [15]. This subtype of stiffness tuning has been previously applied to endoscopic manipulators [16], [17], robotic dolphin tails [18], and by the authors on soft-rigid modules [14], although the mechanism presented here is a novel one compared to previous examples. Here we seek to unleash its potential to untether soft-rigid robots by presenting it alongside a corresponding general-purpose differentiable simulation method.

We also present a sea turtle demonstrator robot inspired by previous work in swimming robots [19]–[23], particularly untethered ones [24]–[26]; turtle robots [27]; and differentiable simulation of swimming robots [28]. We were particularly inspired by the work of Baines et al. [29], which applies heat to thermoset polymers to transition a robot between swimming and walking states. The work also bears similarities to recently published work on flagella robots [30], underwater flappers [31], and biological diggers [32], which utilize asymmetric *passive* compliance to generate thrust. We leave a comparison between passive and active stiffness modulation strategies to future work.

In summary, we present

- the design, modeling, and characterization of a new stiffness tuning mechanism using accordion flexures,
- an extension of the FEM-based simulator from [14] that integrates basic hydrodynamics along with soft and rigid materials, cable actuation, and servo joint actuation, and
- SoRiTu, an untethered sea turtle robot fabricated and simulated using the above methods, which harnesses soft-rigid flippers to swim in a novel locomotion style.

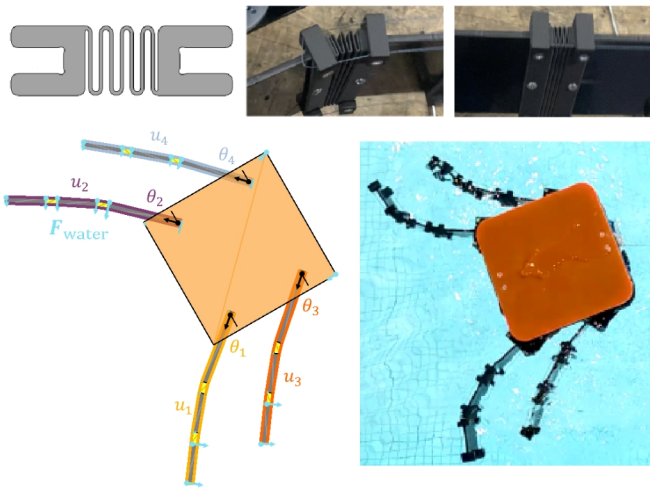

Fig. 1. We present a push puppet-inspired stiffness tuning mechanism, which uses cables and 3D-printed flexures for dramatic stiffness change, and apply it to simulate and fabricate a soft-rigid robotic sea turtle.

* The first two authors contributed equally.
[1] Computer Science, Williams College. jmb15@williams.edu
[2] Computer Science and Artificial Intelligence Laboratory, MIT. zpatt@mit.edu, rus@csail.mit.edu

2023 IEEE/RSJ International Conference on Intelligent Robots and Systems (IROS) | 978-1-6654-9190-7/23/$31.00 ©2023 IEEE | DOI: 10.1109/IROS55552.2023.10341630

II. 3D-Printed Mechanism Design

Inspired by previous work on push puppet-inspired soft-rigid mechanisms [14], we designed the flexure shown at the top of Figure 1. The geometry is a simple accordion structure, which is a well known technique for designing variable stiffness mechanisms in many areas of mechanical engineering [33], [34]. When actively manipulated, the structure can traverse a large stiffness regime when actuated. As a passive structure, the accordion flexure demonstrates highly flexible behavior; when the accordion is actively compressed, it becomes stiffer due to the imposed geometric constraints as the folds of the flexures make contact.

The flexures can be modeled with bending theory for curved beams, as in [35]. We adapt the following equation for the deflection of a curved beam with a small radius of curvature relative to the depth of the flexure,

$$\theta = \frac{nA_m M\pi}{A(RA_m - A)E}, \tag{1}$$

where $A = ht$ is the cross sectional area, $A_m = h\log(\frac{r_o}{r_i})$, R is the (unloaded) radius of curvature, E is Young's Modulus, n is the number of folds of the flexure, M is the bending moment, h and t are the depth and thickness of the flexure, and r_o and r_i are the outer and inner radii respectively. The geometric parameters allow for a broad design space. Here, we chose values that fit with the scale of the forthcoming robot and that resulted in a relatively low stiffness structure. The parameters for this particular design are $h = 88mm$, $t = 0.5mm$, $r_o = 1mm$, $r_i = 0.5mm$. Young's Modulus for Markforged's Onyx material, which was used to print the flexures, is $2.4GPa$. Using these values, we determine that the approximate torsional stiffness of the flexure in its uncompressed state will be $k = 0.16N \cdot m/rad$.

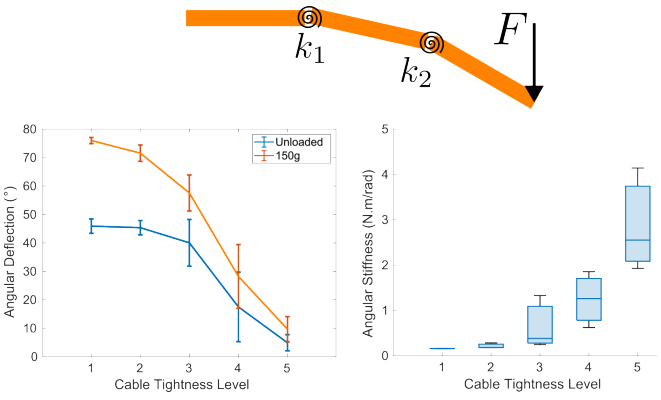

Fig. 2. We characterize the wide range of achievable stiffnesses by hanging masses from several robot limb, as shown in the schematic (top). We measure angular deflection (bottom left) and calculate the net stiffness of a representative beam model (bottom right) for five levels of cable contraction. To account for the effect of gravity, we take the difference between loaded and unloaded cases.

We then created 2D manipulators utilizing two of these flexures in a simple beam-like structure. To modulate the stiffness of the flexures, motor driven cables are used which allow for rapid and efficient stiffness modulation due to the maturity and relative efficiency of motor technology compared to other actuation modalities [36].

To characterize the stiffness tuning property of the beams, we performed a straightforward bending test with a known weight suspended from a cable-actuated beam with two of the flexures. The stiffness of the structure is then varied by setting the motor angle. The deflection is measured under both the loaded and unloaded conditions, and values are displayed in Figure 2. We note that, in a relaxed state, the structure bends nearly 90° under load, whereas in the stiffest state, the average deflection is less than 10°.

Using the deflection information for the individual segments, it was also possible to calculate the individual stiffness of each flexure by assuming linearity and taking the ratio between the loaded and unloaded states. For the loose configuration, we estimate the stiffnesses as $k_1 = 0.17N \cdot m/rad$ and $k_2 = 0.14N \cdot m/rad$, in good agreement with the model. We then calculate the stiffness of the overall structure based on the above, which is plotted in Figure 2 (right). Note the more than order of magnitude difference in stiffness.

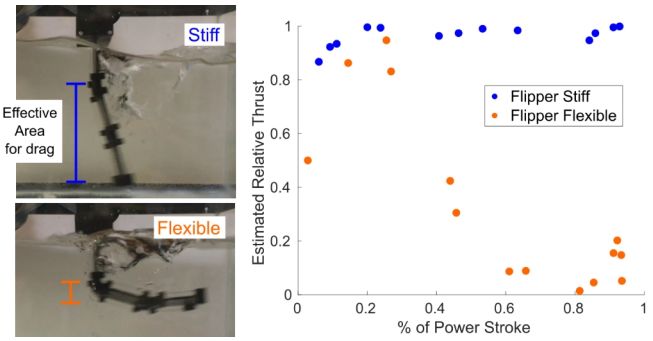

Fig. 3. Left: Snapshots of tests in which the flipper is in a stiff state (top) and flexible state (bottom). Right: Results from several such tests which calculate the area of the flipper that is generating thrust via drag relative to the area of a rigid plate.

Finally, as the beams are to be deployed on an aquatic robot that will perform drag-based rowing, we briefly characterize the interaction between the drag and the stiffness tunable beam, henceforth called a flipper. This was done by suspending the robot above a tank and actuating the limb in a characteristically flexible configuration and in a characteristically rigid one. The deflection of each segment is observed and we calculate an "effective area" as the proportion of the possible cross sectional area that is perpendicular to the velocity of the shoulder joint (with 1 being that of a rigid plate). Since drag scales linearly with area, we plot this term as the "Effective Relative Thrust" in Figure 3 (right) versus the percentage of the power stroke for several trials. From the plots, it is clear that, for the final 60% of the power stroke, the stiff configuration is able to sustain a much larger effective area and therefore a much larger thrust (≈5-10X larger). Switching between these stiff and flexible configurations can therefore serve as the basis for gaits that generate net forward locomotion on a robot.

III. Differentiable Simulation Model

We extend the simulator for push puppet-inspired soft-rigid robots in [14] to incorporate a compatible notion of hydrodynamic drag. This overall framework proves to be an effective way to simulate an untethered soft-rigid robot. We show the output of our simulator in our Supplemtary Video and side by side with a real-world robot in Figure 6.

We model a soft-rigid robot as a multi-body, multi-material finite element mesh. The mesh's nodal positions are assembled into a vector $\boldsymbol{x}$, and its cable contractions and servo joint angles are assembled into vectors $\boldsymbol{u}$ and $\boldsymbol{\theta}$, respectively. To visualize these different parts of the simulation, please see Figure 1, which shows a simulation with five bodies (one base and four arms) with eight actuator degrees of freedom (four cable contractions assembled into $\boldsymbol{u}$ and four servo joint angles assembled into $\boldsymbol{\theta}$.) Cables are drawn as bold colorful lines. Finite elements with low Young's modulus, corresponding to the 3D-printed flexure mechanisms, are drawn in yellow.

In order to enable us to take large timesteps ($h = .0167s$), we employ an implicit physics solver. Specifically, we solve

$$\boldsymbol{x}_k(\boldsymbol{u}_k\boldsymbol{\theta}_k) = \arg\min_{\boldsymbol{x}_k} \left(U(\boldsymbol{u}_k, \boldsymbol{\theta}_k, \boldsymbol{x}_k) + \frac{h^2}{2} \boldsymbol{a}_k^T \boldsymbol{M} \boldsymbol{a}_k \right), \tag{2}$$

using Newton's method with line search, where $\boldsymbol{a}_k$ contains the nodal accelerations discretized using implicit Euler, U is the total potential energy, and $\boldsymbol{M}$ is the mass matrix. This framework is highly modular in the sense that new physical phenomena can be tacked on by adding their energy contribution to U. Each finite element, cable, and revolute joint contributes one of more "spring-like" energy terms to U. By the work-energy principle, the negative derivative of this energy with respect to $\boldsymbol{x}$ is the nodal forces $\boldsymbol{F} = -\frac{\partial U}{\partial \boldsymbol{x}}$ While non-conservative forces, such as friction, cannot be perfectly represented by a potential, recent work has shown enormous success in *approximating* such quantities as well-behaved potentials [37], [38].

In a similar vein, we add to our framework a compatible notion of hydrodynamics, similar to past work in computer graphics like [39]. Here we describe the case for a 2D mesh with nodal positions $\boldsymbol{x}$. For each edge $(\boldsymbol{x}_i, \boldsymbol{x}_j)$, on the oriented outer boundary of the mesh, we calculate an outward facing unit normal $\boldsymbol{n}$ and the edge's "effective velocity" $\boldsymbol{v} = (\boldsymbol{v}_i + \boldsymbol{v}_j)/2$. We call $\boldsymbol{v}_\perp = \max(0, \boldsymbol{v} \cdot \boldsymbol{n})$ the positive component of this velocity perpendicular to the edge. If L is the rest length of this edge, then we have the approximate (2D) volume of water moved by this edge is $L\boldsymbol{v}_\perp$. We can approximate the force imparted by the water on the robot as

$$\boldsymbol{F}_{\text{water}} = -kL\boldsymbol{v}_\perp^2, \tag{3}$$

where k is an empirically determined constant. To simplify our implementation, we can lag this force by one timestep, which allows us to incorporate it into our physics calculations as we would an external force. To account for an external force $\boldsymbol{f}$ on node $\boldsymbol{x}_i$, we can add the energy contribution $-\boldsymbol{f} \cdot \boldsymbol{x}_i$ to the total energy of the system.

A. Modeling Decisions for Real-Time Simulation

We desire a model that strikes a balance between accuracy and efficiency. In order to hit real-time rates, we make several approximations, which all work toward keeping the total number of finite elements low. First, we simulate the real-world 3D robot using a representative 2D cross-section. Second, we model the robot's rigid square-shaped body as two triangular elements. Finally, we distill the complex flexure geometry shown in Figure 1 into similarly simple groups of softer finite elements, drawn in yellow in Figure 6. Our simulation runs at around 200 frames per second on a laptop, which is over three times faster than real-time.

B. Intuitive, Open-Loop Control Interface

We apply our real-time simulator to do open-loop control. We hand-design a library of simple motion primitives, which consist of a sequence of servo targets, and their durations. The user can steer an untethered, sort-rigid robot in real-time by selecting the robot's current primitive motion on the fly.

IV. Demonstrator Robot: SoRiTu

Based on the above stiffness tuning mechanism, we designed an untethered robot called SoRiTu, shown in Figure 1 and this Video[1]. It has two waterproof servos per arm, for a total of eight actuator degrees of freedom Figure 1. Each flipper's larger servo directly actuates a revolute shoulder joint. Each flipper's smaller servo actuates a cable that modulates stiffness. SoRiTu is capable of elementary motions including swimming straight, turning, and turning in place, which can be chained together as shown in Figure 7.

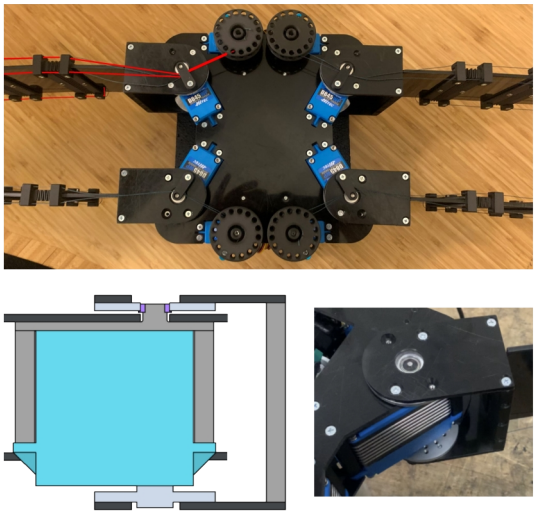

Fig. 4. Above: The underside of SoRiTu. Cables responsible for controlling flipper stiffness are routed around the shoulder joint and onto 3D-printed spools. The top left cable's routing path is highlighted in red. Below: Design and detail of the SoRiTu's shoulder joint. The off-the-shelf waterproof servo responsible for actuating the shoulder is sandwiched between the two body plates using 3D-printed standoffs, and it doubles as a structural element. An idler is created using a flanged bearing, which is colored purple on the left.

[1] https://youtu.be/VEbXM5JIOhs

A. Robot Materials

SoRiTu's shoulders and cables are actuated by Hitec D845WP and D646WP IP67 waterproof servos respectively, shown in Figure 4. We add a ProModeler PDRS22R-15T servo horn to the larger D845WP. The servo cables pass into a Polycase ML-24F IP68 waterproof polycarbonate box, where they are connected to a Pololu Mini Maestro 12-Channel USB Servo Controller, which is powered by two KeepPower 18650 3000mAh Protected High Discharge lithium ion batteries.

SoRiTu's body and flipper plates were waterjet from acetal (Delrin®). The flipper flexures and other nonplanar parts were printed from Onyx on a Markforged X7. The servo idlers were waterjet from aluminum, tapped, and reamed to press in bearings from Avid Racing Concepts LLC. The buoyancy plates were waterjet from styrofoam and painted black with acrylic paint.

B. Robot Characterization

We characterized SoRiTu through pool testing. We hand-specified motion primitives for behaviors corresponding to swimming straight (shown in Figures 5, 6 and 8), turning, and turning in place (shown in Figure 6). Roughly characterizing the performance of these gaits, we find that the average velocity of a single straight cycle is about 5 cm/s while the average angular velocity of a turning cycle is about 8°/s. However, these values are well below average speeds observed through multiple cycles due to the nonlinearities inherent in drag-based swimming. Over multiple cycles, we found that the robot could move in a straight line at roughly 0.2 m/s which is ~ 1 body lengths per second (blps). After testing the behaviors individually, we chained many together to perform more complex trajectories. An example of such a trajectory is shown in Figure 7. Finally, we performed experiments where the weight of the robot was balanced with the buoyant force and showed that the SoRiTu was capable of submersed swimming.

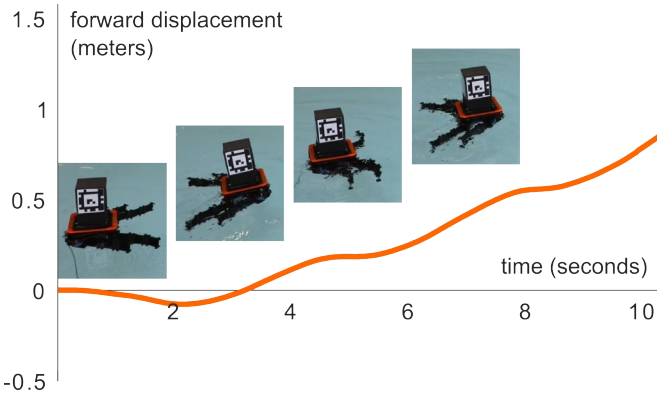

Fig. 5. SoRiTu softens its flippers to minimize the negative thrust of its recovery stroke and stiffens its flippers to maximize the thrust of its power stroke. This plot we visualize the displacement profile of SoRiTu's straight line swimming motion. The flat regions of the plot correspond to recover stokes, and the inclined regions correspond to power strokes. Note that the initial backwards movement is due tocompares the robot bringing its flippers forward in preparation for the power stroke.

The robot's swimming speed compares favorably to recent soft swimming robots [29], [40], [41], especially to untethered examples [28] (0.5 blps), [42] (0.34 blps), [26] (0.3 blps), and [24] (0.15 blps). This is accomplished despite the lack of a roll degree of freedom for the shoulder joints. The recovery stroke's negative thrust is reduced by effective use of cable-driven stiffness modulation, enabling SoRiTu to swim quickly relative to the state of the art.

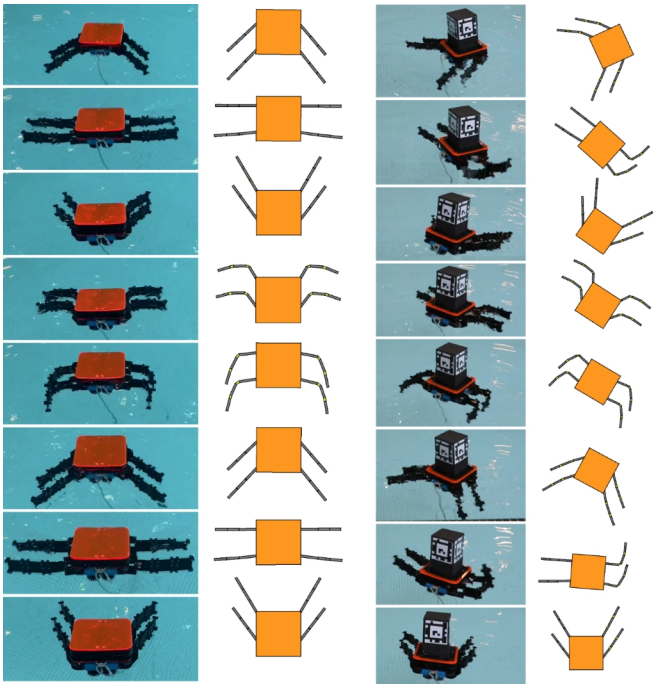

Fig. 6. Snapshots of SoRiTu's straight line swimming (left) and clockwise turn (right) motions shown in reality and in simulation. Time is going up. The simulation captures the salient features of both motions. Please note that the rope shown in the images is just that; a rope. We used the rope to pull the robot back to shore; the rope contains no wires. All power and compute are housed inside the robot.

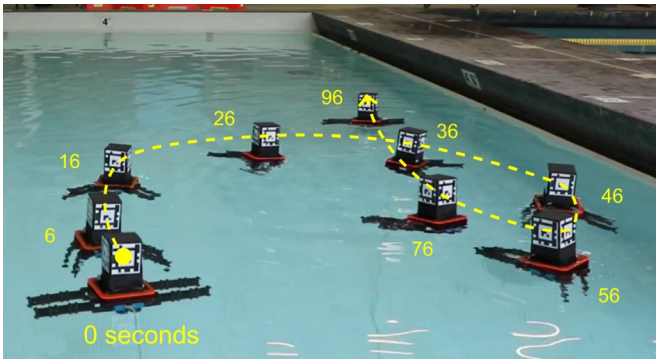

Fig. 7. By composing a sequence of primitive motions, we can command SoRiTu to swim in various 2D trajectories. Here we show overlaid snapshots of a motion sequence designed to make SoRiTu swim in a loop and then to the end of the pool. The timestamp of each snapshot is indicated, along with the qualitative overall trajectory.

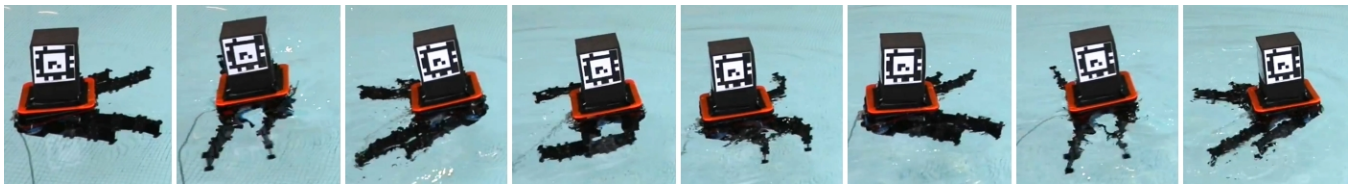

Fig. 8. Side view snapshots of SoRiTu's straight line swimming motion.

V. Discussion and Future Work

We have demonstrated a novel active stiffness tuning mechanism that utilizes an accordion structure between rigid plates. This mechanism has qualitative properties for stiffness tuning that, depending on the application, are improvements over similar mechanisms in the literature. These include no significant length change during operation (contra [16], [18]), much larger joint limits (close to 180° versus 45° for [17]), and a simple design and fabrication process.

A. Closed-loop Control

Our demonstrator robot SoRiTu currently operates in the open loop, as our FEM-based simulator is not fast enough to be run in a model-predictive fashion. We are interested in investigating more efficient modeling approaches, such as those that leverage the GPU [43] to open the door to real-time closed-loop control and more involved tasks.

B. High-fidelity Simulation

Similarly to how it would be interesting to create more inexpensive models to enable real-time control, it would be interesting to create higher fidelity models to enable precise offline trajectory generation and control optimization. Currently, our simulator's treatment of the flexures and the water involves particularly large approximations.

1) Flexures: The complex flexure geometry shown in Figure 1 is represented by a small number of finite elements with low Young's modulus. This yields a model that is much faster than we could ever hope to achieve by modeling the thin flexure geometry directly. It would be interesting to employ a per-element material parameter optimization approach like [44] to do this coarse mesh approximation in an optimal fashion, and achieve a simulation that is both efficient and accurate.

2) Water: There are multiple interesting avenues for improving the fidelity of the water simulation. First, we could take a more classic approach and integrate a fluid simulation based on the Navier-Stokes equations [45]. Alternatively, we could employ physics-constrained deep learning to learn a differentiable model of the water [46], [47].

C. 3D Spatial Trajectories

Additionally, while we showed that SoRiTu is capable of swimming underwater, SoRiTu currently has no way of controlling its height within the water column. To open the door to more exciting 3D motions, future work could integrate buoyancy control [25] or a third roll degree of freedom for the flippers along with more sophisticated control strategies.

VI. Conclusions

We proposed active accordion flexures as a convenient and accessible way of untethering soft rigid robots. We characterized our flexure design and showed how it could be modeled in a differentiable soft-rigid robot simulation framework. We designed and fabricated SoRiTu, a soft-rigid sea turtle robot with push puppet-inspired flippers. SoRiTu's mechanical design used cables to rapidly and dramatically change its flippers stiffness, which enabled multiple swimming motion primitives. We demonstrate SoRiTu's ability to swim in reality and in simulation.

Acknowledgment

We are grateful to the NSF for partial support under Grant EFRI program Grant #1830901. We would also like to thank John Romanishin, Levi Cai, Juan Salazar, and Josie Hughes.

References

[1] H.-I. Kim, M.-W. Han, S.-H. Song, and S.-H. Ahn, "Soft morphing hand driven by sma tendon wire," *Composites Part B: Engineering*, vol. 105, pp. 138–148, 2016.

[2] D. Rus and M. T. Tolley, "Design, fabrication and control of soft robots," *Nature*, vol. 521, no. 7553, pp. 467–475, May 2015.

[3] J. F. Wilson, U. Mahajan, S. A. Wainwright, and L. J. Croner, "A Continuum Model of Elephant Trunks," *Journal of Biomechanical Engineering*, vol. 113, no. 1, pp. 79–84, Feb. 1991.

[4] W. M. KIER and K. K. SMITH, "Tongues, tentacles and trunks: The biomechanics of movement in muscular-hydrostats," *Zoological Journal of the Linnean Society*, vol. 83, no. 4, pp. 307–324, Apr. 1985.

[5] J. A. Mather, "How do octopuses use their arms?" *Journal of Comparative Psychology*, vol. 112, pp. 306–316, 1998.

[6] C. L. Huffard, "Locomotion by Abdopus aculeatus (Cephalopoda: Octopodidae):walking the line between primary and secondary defenses," *Journal of Experimental Biology*, vol. 209, no. 19, pp. 3697–3707, Oct. 2006.

[7] S. I. Rich, R. J. Wood, and C. Majidi, "Untethered soft robotics," *Nature Electronics*, vol. 1, no. 2, pp. 102–112, 2018.

[8] C. Majidi, "Soft-Matter Engineering for Soft Robotics," *Advanced Materials Technologies*, vol. 4, no. 2, p. 1800477, 2019.

[9] G. Sumbre, G. Fiorito, T. Flash, and B. Hochner, "Octopuses Use a Human-like Strategy to Control Precise Point-to-Point Arm Movements," *Current Biology*, vol. 16, no. 8, pp. 767–772, Apr. 2006.

[10] ——, "Motor control of flexible octopus arms," *Nature*, vol. 433, no. 7026, pp. 595–596, Feb. 2005.

[11] L. Wang, Y. Yang, Y. Chen, C. Majidi, F. Iida, E. Askounis, and Q. Pei, "Controllable and reversible tuning of material rigidity for robot applications," *Materials Today*, vol. 21, no. 5, pp. 563–576, Jun. 2018.

[12] M. Manti, A. Pratesi, E. Falotico, M. Cianchetti, and C. Laschi, "Soft assistive robot for personal care of elderly people," in *2016 6th IEEE International Conference on Biomedical Robotics and Biomechatronics (BioRob)*, Jun. 2016, pp. 833–838.

[13] T. S. Dahl and M. N. K. Boulos, "Robots in Health and Social Care: A Complementary Technology to Home Care and Telehealthcare?" *Robotics*, vol. 3, no. 1, pp. 1–21, Mar. 2014.

[14] J. M. Bern, L. Z. Yañez, E. Sologuren, and D. Rus, "Contact-rich soft-rigid robots inspired by push puppets," in *2022 IEEE 5th International Conference on Soft Robotics (RoboSoft)*, 2022, pp. 607–613.

[15] Y. Yang, Y. Li, and Y. Chen, "Principles and methods for stiffness modulation in soft robot design and development," *Bio-Design and Manufacturing*, vol. 1, no. 1, pp. 14–25, 2018.

[16] T. M. Huh, Y.-J. Park, and K.-J. Cho, "Design and analysis of a stiffness adjustable structure using an endoskeleton," *International Journal of Precision Engineering and Manufacturing*, vol. 13, pp. 1255–1258, 2012.

[17] Y.-J. Kim, S. Cheng, S. Kim, and K. Iagnemma, "A stiffness-adjustable hyperredundant manipulator using a variable neutral-line mechanism for minimally invasive surgery," *IEEE transactions on robotics*, vol. 30, no. 2, pp. 382–395, 2013.

[18] Y.-J. Park, T. M. Huh, D. Park, and K.-J. Cho, "Design of a variable-stiffness flapping mechanism for maximizing the thrust of a bio-inspired underwater robot," *Bioinspiration & biomimetics*, vol. 9, no. 3, p. 036002, 2014.

[19] M. Porez, F. Boyer, and A. J. Ijspeert, "Improved lighthill fish swimming model for bio-inspired robots: Modeling, computational aspects and experimental comparisons," *The International Journal of Robotics Research*, vol. 33, no. 10, pp. 1322–1341, 2014.

[20] A. Arienti, M. Calisti, F. Giorgio-Serchi, and C. Laschi, "Poseidrone: design of a soft-bodied rov with crawling, swimming and manipulation ability," in *2013 OCEANS-San Diego*. IEEE, 2013, pp. 1–7.

[21] J. Shintake, V. Cacucciolo, H. Shea, and D. Floreano, "Soft Biomimetic Fish Robot Made of Dielectric Elastomer Actuators," *Soft Robotics*, vol. 5, no. 4, pp. 466–474, Aug. 2018.

[22] M. A. Robertson, F. Efremov, and J. Paik, "RoboScallop: A Bivalve Inspired Swimming Robot," *IEEE Robotics and Automation Letters*, vol. 4, no. 2, pp. 2078–2085, Apr. 2019.

[23] A. Crespi, K. Karakasiliotis, A. Guignard, and A. J. Ijspeert, "Salamandra Robotica II: An Amphibious Robot to Study Salamander-Like Swimming and Walking Gaits," *IEEE Transactions on Robotics*, vol. 29, no. 2, pp. 308–320, Apr. 2013.

[24] R. K. Katzschmann, A. D. Marchese, and D. Rus, "Hydraulic autonomous soft robotic fish for 3d swimming," in *Experimental Robotics*. Springer, 2016, pp. 405–420.

[25] A. D. Marchese, C. D. Onal, and D. Rus, "Autonomous soft robotic fish capable of escape maneuvers using fluidic elastomer actuators," *Soft robotics*, vol. 1, no. 1, pp. 75–87, 2014.

[26] Z. Wu, J. Yu, J. Yuan, and M. Tan, "Towards a gliding robotic dolphin: design, modeling, and experiments," *IEEE/ASME Transactions on Mechatronics*, vol. 24, no. 1, pp. 260–270, 2019.

[27] S.-H. Song, M.-S. Kim, H. Rodrigue, J.-Y. Lee, J.-E. Shim, M.-C. Kim, W.-S. Chu, and S.-H. Ahn, "Turtle mimetic soft robot with two swimming gaits," *Bioinspiration & biomimetics*, vol. 11, no. 3, p. 036010, 2016.

[28] X. Huang, Z. J. Patterson, A. P. Sabelhaus, W. Huang, K. Chin, Z. Ren, M. K. Jawed, and C. Majidi, "Design and closed-loop motion planning of an untethered swimming soft robot using 2d discrete elastic rods simulations," *Advanced Intelligent Systems*, vol. 4, no. 10, p. 2200163, 2022.

[29] R. Baines, S. K. Patiballa, J. Booth, L. Ramirez, T. Sipple, A. Garcia, F. Fish, and R. Kramer-Bottiglio, "Multi-environment robotic transitions through adaptive morphogenesis," *Nature*, vol. 610, no. 7931, pp. 283–289, Oct. 2022, number: 7931 Publisher: Nature Publishing Group. [Online]. Available: https://www.nature.com/articles/s41586-022-05188-w

[30] K. Diaz, T. L. Robinson, Y. O. Aydin, E. Aydin, D. I. Goldman, and K. Y. Wan, "A minimal robophysical model of quadriflagellate self-propulsion," *Bioinspiration & Biomimetics*, vol. 16, no. 6, p. 066001, 2021.

[31] M. Sharifzadeh, Y. Jiang, and D. M. Aukes, "Reconfigurable curved beams for selectable swimming gaits in an underwater robot," *IEEE Robotics and Automation Letters*, vol. 6, no. 2, pp. 3437–3444, 2021.

[32] S. Chopra, D. Vasile, S. Jadhav, M. T. Tolley, and N. Gravish, "Toward robotic sensing and swimming in granular environments using underactuated appendages," *Advanced Intelligent Systems*, p. 2200404, 2023.

[33] I. K. Kuder, A. F. Arrieta, W. E. Raither, and P. Ermanni, "Variable stiffness material and structural concepts for morphing applications," *Progress in Aerospace Sciences*, vol. 63, pp. 33–55, 2013.

[34] G. C. Engelmayr Jr, M. Cheng, C. J. Bettinger, J. T. Borenstein, R. Langer, and L. E. Freed, "Accordion-like honeycombs for tissue engineering of cardiac anisotropy," *Nature materials*, vol. 7, no. 12, pp. 1003–1010, 2008.

[35] A. P. Boresi, R. J. Schmidt, O. M. Sidebottom *et al.*, *Advanced mechanics of materials*. Wiley New York, 1985, vol. 6.

[36] N. El-Atab, R. B. Mishra, F. Al-Modaf, L. Joharji, A. A. Alsharif, H. Alamoudi, M. Diaz, N. Qaiser, and M. M. Hussain, "Soft actuators for soft robotic applications: a review," *Advanced Intelligent Systems*, vol. 2, no. 10, p. 2000128, 2020.

[37] M. Li, Z. Ferguson, T. Schneider, T. Langlois, D. Zorin, D. Panozzo, C. Jiang, and D. M. Kaufman, "Incremental potential contact: Intersection-and inversion-free, large-deformation dynamics," *ACM transactions on graphics*, 2020.

[38] M. Li, D. M. Kaufman, and C. Jiang, "Codimensional incremental potential contact," *arXiv preprint arXiv:2012.04457*, 2020.

[39] X. Tu and D. Terzopoulos, "Artificial fishes: Physics, locomotion, perception, behavior," in *Proceedings of the 21st annual conference on Computer graphics and interactive techniques*, 1994, pp. 43–50.

[40] J. Fan, S. Wang, Q. Yu, and Y. Zhu, "Swimming Performance of the Frog-Inspired Soft Robot," *Soft Robotics*, vol. 7, no. 5, pp. 615–626, Oct. 2020, publisher: Mary Ann Liebert, Inc., publishers. [Online]. Available: https://www.liebertpub.com/doi/full/10.1089/soro.2019.0094

[41] D. Q. Nguyen and V. A. Ho, "Anguilliform Swimming Performance of an Eel-Inspired Soft Robot," *Soft Robotics*, vol. 9, no. 3, pp. 425–439, Jun. 2022, publisher: Mary Ann Liebert, Inc., publishers. [Online]. Available: https://www.liebertpub.com/doi/full/10.1089/soro.2020.0093

[42] G. Li, X. Chen, F. Zhou, Y. Liang, Y. Xiao, X. Cao, Z. Zhang, M. Zhang, B. Wu, S. Yin, Y. Xu, H. Fan, Z. Chen, W. Song, W. Yang, B. Pan, J. Hou, W. Zou, S. He, X. Yang, G. Mao, Z. Jia, H. Zhou, T. Li, S. Qu, Z. Xu, Z. Huang, Y. Luo, T. Xie, J. Gu, S. Zhu, and W. Yang, "Self-powered soft robot in the Mariana Trench," *Nature*, vol. 591, no. 7848, pp. 66–71, Mar. 2021, number: 7848 Publisher: Nature Publishing Group. [Online]. Available: http://www.nature.com/articles/s41586-020-03153-z

[43] L. Lan, G. Ma, Y. Yang, C. Zheng, M. Li, and C. Jiang, "Penetration-free projective dynamics on the gpu," *ACM Transactions on Graphics (TOG)*, vol. 41, no. 4, pp. 1–16, 2022.

[44] D. Hahn, P. Banzet, J. M. Bern, and S. Coros, "Real2sim: Visco-elastic parameter estimation from dynamic motion," *ACM Transactions on Graphics (TOG)*, vol. 38, no. 6, pp. 1–13, 2019.

[45] J. Tan, Y. Gu, G. Turk, and C. K. Liu, "Articulated swimming creatures," *ACM Transactions on Graphics (TOG)*, vol. 30, no. 4, pp. 1–12, 2011.

[46] N. Wandel, M. Weinmann, and R. Klein, "Teaching the incompressible navier–stokes equations to fast neural surrogate models in three dimensions," *Physics of Fluids*, vol. 33, no. 4, p. 047117, 2021.

[47] J. Z. Zhang, Y. Zhang, P. Ma, E. Nava, T. Du, P. Arm, W. Matusik, and R. K. Katzschmann, "Learning material parameters and hydrodynamics of soft robotic fish via differentiable simulation," *arXiv preprint arXiv:2109.14855*, 2021.